Detection of Single Mammalian Cells by High-Resolution Magnetic Resonance Imaging

Stephen J. Dodd,* Mangay Williams,* Joseph P. Suhan,† Donald S. Williams,* Alan P. Koretsky,*† and Chien Ho*†

*Pittsburgh NMR Center for Biomedical Research and †Department of Biological Sciences, Carnegie Mellon University, Pittsburgh, Pennsylvania 15213 USA

ABSTRACT This study reports the detection of single mammalian cells, specifically T cells (T lymphocytes) labeled with dextran-coated superparamagnetic iron oxide particles, using magnetic resonance microscopy. Size amplification due to sequestration of the superparamagnetic particles in vacuoles enhances contrast in localized areas in high-resolution magnetic resonance imaging. Magnetic resonance images of samples containing differing concentrations of T cells embedded in 3% gelatin show a number of dark regions due to the superparamagnetic iron oxide particles, consistent with the number predicted by transmission electron microscopy. Colabeling of T cell samples with a fluorescent dye leads to strong correlations between magnetic resonance and fluorescence microscopic images, showing the presence of the superparamagnetic iron oxide particles at the cell site. This result lays the foundation for our approach to tracking the movement of a specific cell type in live animals and humans.

INTRODUCTION

A major goal of modern imaging techniques is to track the distribution and movement of specific types of cells in physiological systems. Although light microscopic techniques are very useful for optically transparent specimens, they clearly are limited for opaque samples such as tissues and organs in humans. Thus, the ability to track the movement of cells in animals or humans using the noninvasive method of magnetic resonance imaging (MRI) is likely to have an impact not only in cell biology, but also in the diagnosis and management of many disease processes, such as organ rejection in organ transplantation, adhesion of natural killer cells to tumors, and homing of lymphocytes to lymph nodes. We have chosen T cells, the primary effector cells in acute graft rejection, as a model system for visualizing single cells by MRI. The homing of T cells to the site of graft rejection is a major focus in the field of transplantation immunology (Picker and Butcher, 1992). Lymphocytes and other mediators of rejection, such as macrophages, are believed to be attracted to the rejection site by damaged capillary endothelium of the transplanted solid-organ grafts, cellular fragments from grafts, or secreted products. If the early accumulation of T cells and/or macrophages in the graft can be detected with MRI techniques through intracellular incorporation of a MRI contrast agent, such as dextran-coated superparamagentic iron oxide (SPIO) particles, this may provide an alternative to the highly invasive biopsy procedure, the current method of choice for detecting organ rejection in organ transplantation. Our approach is to label T cells by endocytosis ex vivo, re-introduce the labeled T cells into an animal, and then track the movement of the labeled T cells by MRI. The movement of any type of cell could be monitored by MRI methodology in live animals or humans, provided that a sufficient amount of an appropriate MR contrast agent can be incorporated into a given type of cell without disturbing its functional properties.

The use of dextran-coated SPIO particles as a tissue-specific MRI contrast agent is well established (Ghosh et al., 1990; Bulte et al., 1992; Weissleder et al., 1992, 1996; Yeh et al., 1993, 1995; Schoepf et al., 1998). It has also been shown previously that SPIO particles can be incorporated into rat T cells by endocytosis (Yeh et al., 1993), the functional properties of SPIO-labeled T cells are not altered (Yeh et al., 1993), T cells labeled with dextran-coated SPIO particles can produce detectable intensity changes in an in vitro model (Yeh et al., 1993), and these labeled cells can be tracked in vivo with MRI in a tissue inflammation model in the rat testicle (Yeh et al., 1995). Lauterbur et al. (1986) have also shown that small paramagnetic particles may be detected using MR microscopy and that the large magnetic susceptibility of these particles can affect a much larger region of the image than is suggested by the actual size of the particle, e.g., magnetite particles appear in MR images on the order of 50× larger than their actual size.

In the present work, we demonstrate that the superparamagnetic effect of single SPIO-labeled T cells can be detected using high-resolution MRI. Endocytosis of SPIO particles by T cells leads to the accumulation of SPIO particles in phagocytic vacuoles. Due to the accumulation of SPIO particles, MR enhancement occurs over a distance much larger than the vacuole itself, thus enabling the presence of single T cells to be imaged at a resolution achievable by MRI.

Received for publication 16 June 1998 and in final form 11 September 1998.

Address reprint requests to Dr. Chien Ho, Department of Biological Sciences, Carnegie Mellon University, 4400 Fifth Avenue, Pittsburgh, PA 15213. Tel.: 412-268-3395; Fax: 412-268-7083; E-mail: chienho@andrew.cmu.edu.

0006-3495/99/01/103/07 $2.00

MATERIALS AND METHODS

Preparation of SPIO Particles

Dextran-coated SPIO particles were synthesized in our laboratory according to Palmacci and Josephson (1993) by reacting a high concentration of dextran T-10 (Sigma, St. Louis, MO) with ferric chloride and ferrous chloride in aqueous solution. The particles were then purified (Molday and Mackenzie, 1982). Quantitative determination of iron in the particle suspension was performed for all samples using a spectrophotometric method (Papisov et al., 1993). Dextran concentration was determined by the phenol/sulfuric acid method (Dubois et al., 1956). Iron core size was measured with transmission electron microscopy (TEM). Mean diameter of whole particles (including the dextran coating) was measured by laser light-scattering studies.

Isolation of T cells and labeling with SPIO particles

T cells were isolated from lymph nodes of Fischer 344 rats by the nylon wool column technique (Litvin and Rosensireich, 1984; Yeh et al., 1993). Isolated T cells were cultured in reconstituted RPMI 1640 culture medium with 10% fetal calf serum under 5% CO_2 at 37°C. Cell labeling was accomplished by adding the filter-sterilized SPIO particles (2 mg Fe/10 $\times$ 10^6 cells) to the culture medium. The labeled cells were incubated for 40 h, then recovered with three washes with phosphate-buffered saline (PBS) by centrifugation at 400 $\times$ g. Location of SPIO particles in the T cells and estimation of particle loading were carried out by TEM measurements. For details, refer to Yeh et al. (1993, 1995).

Electron microscopy measurements

Preparation of samples for the determination of iron core diameters of SPIO particles and uptake of SPIO particles by T cells were as follows: SPIO particles having a concentration of 1 mg Fe/ml were embedded in 3% gelatin in PBS. A small portion of the gel sample was fixed in 2% glutaraldehyde buffered with PBS, then washed in several changes of PBS and dehydrated in a series of ethanol solutions (50%, 70%, 80%, 90%, and 100%). After exposure to propylene oxide, the sample was infiltrated overnight in a 1:1 mixture of propylene oxide and Epon-Araldite (EMS, Fort Washington, PA). The samples were then infiltrated in 100% Epon-Araldite for 8 h, placed in embedding molds, and polymerized in a 60°C oven for 48 h.

T cells were pelleted and fixed for at least 30 min in 2% glutaraldehyde buffered with PBS. The pellets were washed in several changes of PBS, postfixed in 0.5% OsO_4 buffered with PBS for 15 min, and washed again in several changes of distilled water. The samples were then dehydrated and infiltrated with Epon-Araldite resin as described above for SPIO particles.

The samples for TEM measurements were sectioned using a diamond knife on a Reichert-Jung Ultracut-E ultramicrotome. Thin sections (100 nm) were picked up on copper grids and coated with carbon. The sections were viewed on a Hitachi 7100 transmission electron microscope at 50 keV. Images were recorded with an AMT Advantage 10 Image Acquisition System using a Kodak Megaplus 1.6i CCD camera system (1024 $\times$ 1024 TIFF format) as a plug-in utilizing National Institutes of Health Image software.

Magnetic resonance measurements

The relaxivities, R_1 (spin-lattice relaxation rate, $1/T_1$ per mole of Fe in SPIO) and R_2 (spin-spin relaxation rate, $1/T_2$ per mole of Fe in SPIO) were measured at 4.7 T using a Bruker Biospec Avance-DBX instrument (Bruker Instruments, Inc., Billerica, MA). Relaxation measurements were made on samples of labeled and unlabeled T cells prepared by mixing a pellet containing 10 $\times$ 10^6 cells with 1 ml gelatin (3% w/w in water). T_1 relaxation times were measured using an inversion recovery sequence. T_2 relaxation times for bulk labeled T cell samples were measured using a Carr-Purcell-Meiboom-Gill pulse sequence with an inter-180° pulse interval of 2 ms. T_2 values of SPIO-labeled T cell phantoms with concentrations of 10 $\times$ 10^6 cells/ml showed a 50% reduction compared to unlabeled cells. Using the T_2 measured in labeled cells and the R_2 relaxivity data, reported in Table 1 for free SPIO particles in suspension, we have estimated the iron concentration in the cells to be 0.05 μg Fe/1 $\times$ 10^6 cells.

High-resolution MR imaging was performed on various T cell samples using a 7-T/15-cm Bruker Biospec Avance-DBX instrument equipped with a 4.3-cm microimaging gradient set. For the samples contained in 5-mm inner diameter tubes, a 3-turn solenoid coil was used as the transceiver. The imaging protocol consisted of a 2DFT (2-dimensional Fourier transform) gradient-echo image with long echo time (TE) (usually 30–40 ms) for T_2^* weighting. In all the images, the slice plane had one axis parallel to the main magnetic field (z-direction) in order to enhance local susceptibility effects (Callaghan, 1990). For microscope slide imaging, a rectangular surface coil was used for excitation of a long strip of the sample. Using a gradient-echo sequence, 2D MR imaging of the same regions was performed as soon as possible (within 48 h) after taking the fluorescence images in order to minimize any possible cell displacement caused by water loss in the gel due to evaporation, which occurs even with sealant. Gradient-echo sequences using TR/TE = 1000/40 ms and FA = 45° (where TR is recovery time and FA is flip angle) with no slice selection were used for image acquisition. Resolutions achieved for these experiments were typically on the order of 25-μm isotropic.

Fluorescence microscopy imaging measurements

For comparative fluorescence microscopy and MRI studies, SPIO-labeled T cells were colabeled with the fluorescent lipophilic carbocyanine dye, DiI (1,1-di-octadecyl-3,3,3′,3′-tetramethyl-lindocarbocyanine perchlorate) (Molecular Probes, Eugene, OR). A 0.5% (w/v) DiI stock solution in 1:1 ethanol/DMSO was used to prepare a 0.025% (w/v) DiI solution with reconstituted RPMI 1640 solution. T cells were colabeled by incubating SPIO-labeled T cells recovered from a 40-h cell culture in 0.025% DiI/RPMI-1640 medium for 30 min under 5% CO_2 at 37°C (Yeh et al., 1995). Colabeled T cells were recovered again after three washes with PBS by centrifugation at 400 $\times$ g. Thin samples of colabeled T cells were prepared on microscope slides with 10 μl samples of 5 $\times$ 10^6 T cells/ml in 3% gelatin spread evenly beneath either a 22 $\times$ 22 mm or an 18 $\times$ 18 mm coverslip. A sealant was used around the edges of the coverslip to avoid drying of samples. For comparison, similar samples were also prepared with T cells labeled with only DiI. Fluorescence images of a specified area were obtained at 10$\times$ magnification using a BX 60 fluorescence microscope equipped with an automatic exposure system (Olympus, Tokyo).

RESULTS

Electron microscopy studies

Fig. 1 shows TEM results from a T cell sample labeled with dextran-coated SPIO particles. Incorporation of the SPIO particles into phagocytic vacuoles of T cells by endocytosis can be seen. The diameters of the individual particles in the phagocytic vacuole were measured by TEM and found to be

TABLE 1 Physical properties of dextran-coated SPIO particles

Iron core diameter	4.0–7.5 nm
Whole particle diameter*	30.0 nm
R_1	4.80 $\times$ 10^4 $M^{-1}s^{-1}$
R_2	12.8 $\times$ 10^4 $M^{-1}s^{-1}$

*Obtained from a laser light scattering apparatus (Model N4 plus multiangle submicron particle analyzer, Coulter, Miami, FL) through the courtesy of Dr. Leaf Huang of the University of Pittsburgh School of Medicine.

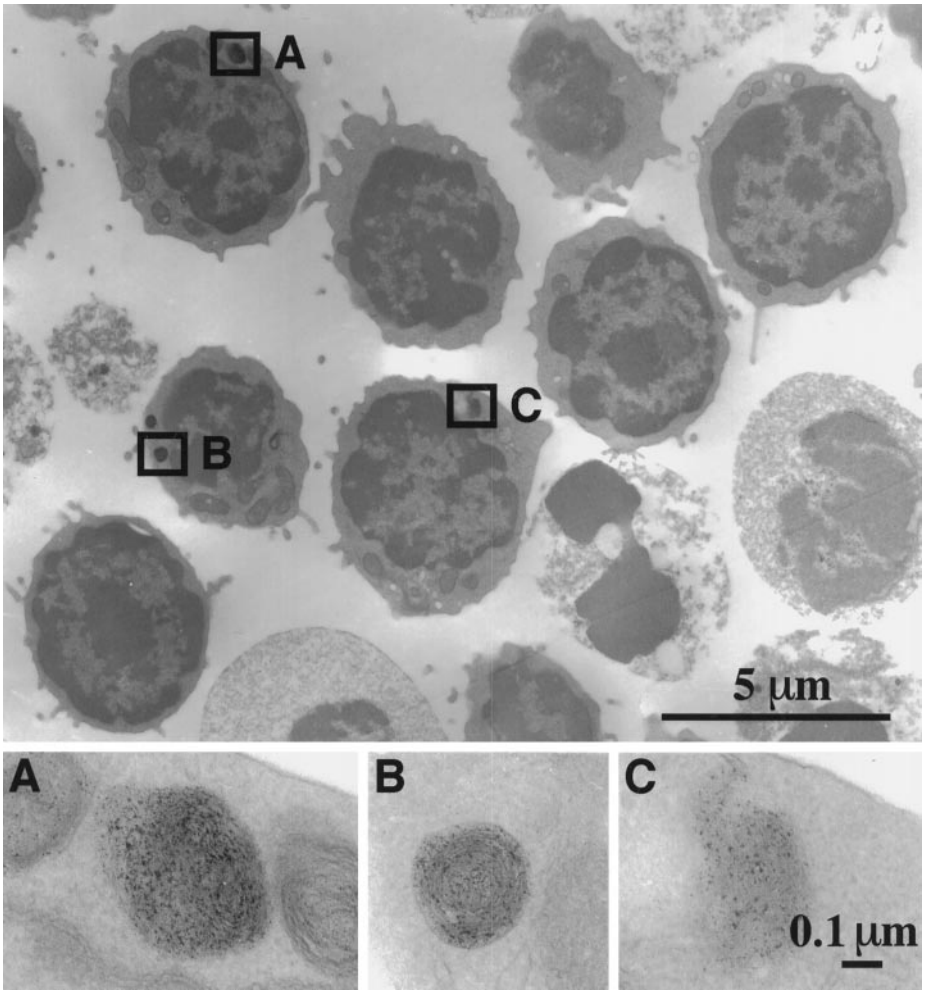

FIGURE 1 Representative TEM image showing accumulation of SPIO particles inside the phagocytic vacuoles of T cells. Regions of the cells containing the particles are shown magnified below the main image. Approximately 20% of the T cells were labeled with SPIO particles by endocytosis under our experimental conditions as shown by TEM. That the accumulated particles essentially act as a single larger particle with paramagnetic properties is one of the advantages of cell labeling via endocytosis.

consistent with the particle size of SPIO (Table 1). The dense packing of SPIO particles in phagocytic vacuoles should, in principle, lead to a larger local magnetic field, i.e., one resulting in higher contrast in MR images, than is available when the contrast agent is in the free state or evenly distributed throughout the cell volume. The labeling efficiency (percentage of cells labeled with SPIO particles) determined from a field containing a large number of cells was approximately 20%.

Magnetic resonance studies

We believe that a key to detecting low concentrations of labeled T cells by MRI is high spatial resolution. Our MRI measurements have shown that a concentration of 10×10^6 labeled T cells/ml with a 20% labeling efficiency (estimated from TEM data) gives a reduction of spin-spin relaxation time (T_2) on the order of 50% at 4.7 T. In such a sample, for every volume of $100 \times 100 \times 100$ μm, we would expect to find two labeled T cells, on average, or a single cell in a volume of $50 \times 100 \times 100$ μm. Assuming the particles are uniformly distributed, images at voxel sizes down to $50 \times 100 \times 100$ μm should have the same concentration of labeled cells as that of the bulk sample and should behave like the bulk sample. However, at resolutions below this threshold, voxels containing a labeled cell should have a much higher paramagnetic label concentration than voxels not containing a labeled cell, and so should lead to enhanced image contrast. In general, a necessary condition for the MR detection of individual labeled cells in a sample of uniformly distributed labeled cells is an image resolution high enough that the number of image voxels per unit volume is greater than the number of labeled cells per unit volume. Further increases in image resolution will lead to higher image contrast.

Fig. 2, *A-F*, shows T_2^*-weighted MR images with $50 \times 50 \times 100$ μm resolution (4×10^6 voxels/ml) of labeled and unlabeled T cell samples with concentrations of 2×10^6, 1×10^6, and 0.25×10^6 T cells/ml. Comparing the labeled cell images of Fig. 2 *A*, *C*, and *E* with the unlabeled cell images of Fig. 2 *B*, *D*, and *F* clearly shows the samples containing SPIO-labeled cells giving rise to punctate loss of signal, the quantity of which decreases with a decrease in cell concentration. In most of the samples with unlabeled cells, one or two small dots can be seen, due most probably to the presence of small air bubbles.

The idea of increasing image contrast by increasing spatial resolution was tested with gradient-echo images (TR/TE = 1000/40 ms) in a sample of 0.25×10^6 cells/ml with the in-plane resolution maintained at 50 μm, but with in-

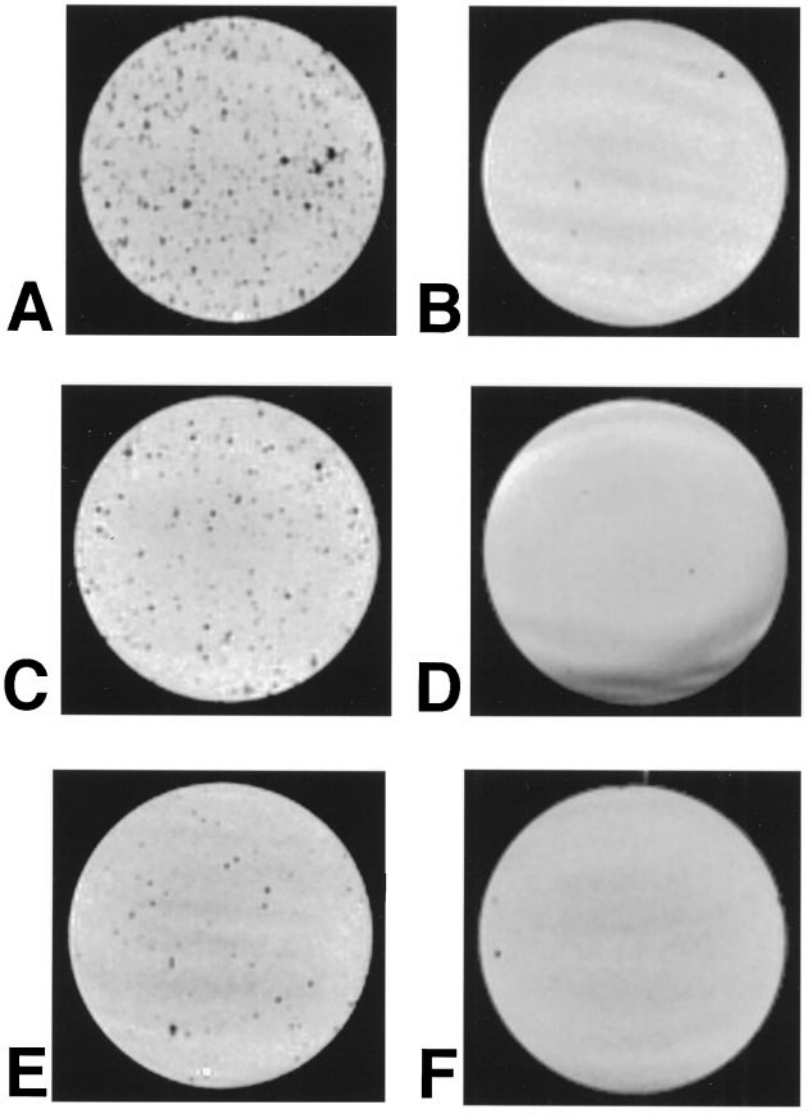

FIGURE 2 Gradient-echo images showing SPIO-labeled (*A*, *C*, *E*) and unlabeled (*B*, *D*, *F*) T cell samples. Cell concentrations were as follows: (*A*) and (*B*), 2.0×10^6 T cells/ml; (*C*) and (*D*), 1.0×10^6 T cells/ml; (*E*) and (*F*), 0.25×10^6 T-cells/ml. Imaging parameters were as follows: TR/TE = 1000/30 ms; FA = 45°; matrix size = 128 × 128; FOV = 6.4 mm; slice thickness = 100 μm; in-plane resolution = 50 × 50 μm; acquisition bandwidth = 20 kHz; number of averages = 8; experiment time = 17 min. In each case, the direction of the read gradient was from left to right and the phase-encoding direction was vertical. Bulk samples for high-resolution MRI studies were prepared in 1-ml plastic syringes by suspending labeled and unlabeled T cell samples in 3% gelatin.

creasing slice thickness from 0.1 mm (a voxel of 2.5×10^{-4} mm^3) through 0.5 mm (a voxel of 12.5×10^{-4} mm^3) in increments of 0.1 mm. Fig. 3 shows a plot of the MR signal intensity decrease due to the presence of SPIO-labeled T cells as a function of voxel size. The image contrast, as measured by the ratio of the intensity within a voxel containing a labeled cell to that of a group of surrounding voxels, varied from 33% to 2%. Another set of MR images was taken with a constant resolution of 50 × 50 × 100 μm but with TE values of 40, 30, 20, 13, and 9 ms (Fig. 4). The MR signal intensity is seen to decrease, due to the presence of SPIO particles, from 33% at TE of 40 ms down to 11% at a TE value of 9 ms, illustrating the increase of contrast by increasing the echo time.

The benefit of labeling cells by endocytosis, which leads to dense packing of a large number of SPIO particles into a phagocytic vacuole, is evident from the MR image of a microscope slide preparation as shown in Fig. 5 *A*. Microscope slides were prepared containing SPIO-labeled T cells in 3% gelatin and imaged using a T_2^*-weighted gradient-echo sequence. The in-plane resolution was 25 × 50 μm. Slice selection was not used because of the very thin sample, allowing the sample to determine the thickness of the

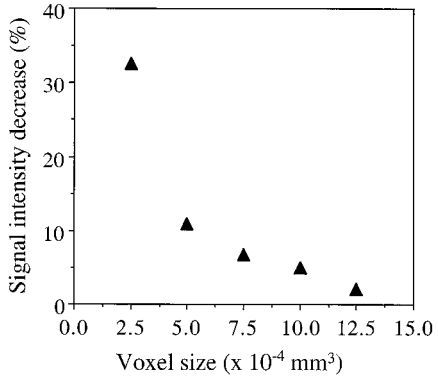

FIGURE 3 Plot showing MR signal intensity decrease due to the presence of SPIO particles as a function of voxel size.

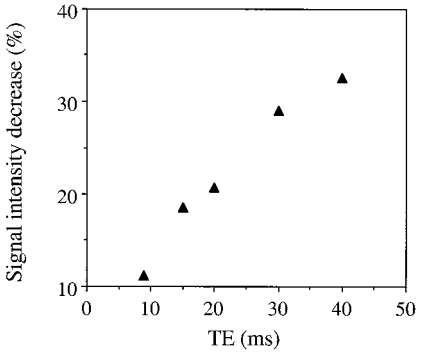

FIGURE 4 Plot showing MR signal intensity decrease due to the presence of SPIO particles as a function of echo time (TE).

slice. It was estimated that the sample thickness was on the order of 25 μm, assuming that a 10 μl sample was spread evenly beneath a 22 $\times$ 22 mm coverslip. Fig. 5 *A* shows an MR image (32 $\times$ 10^6 voxels/ml) of a sample of 10 $\times$ 10^6 T cells/ml labeled with SPIO. This is compared with a sample containing free SPIO particles at a concentration of 1.0 μg Fe/ml in Figure 5B, twice the amount of SPIO present in a sample of 10 $\times$ 10^6 T cells/ml. Even though the sample containing the free SPIO particles has twice the iron concentration of the labeled T cell sample, no dark spots are seen in the MR image because of the relatively weak magnetic field produced by the individual particles. In the cell, because of the packing of a large number of these particles in the vacuole, a much higher field appears to be produced.

That the dark spots in MR images correspond to the locations of single labeled T cells is supported by the excellent correlation of the measured spot count with that calculated from the sample cell concentration. The number of cells within a region of 1 $\times$ 1 mm cross-section of the sample used for Fig. 5 *A* is calculated as 50 labeled cells (assuming 20% labeling efficiency). Inside such an area from the image in Fig. 5 *A*, we counted 40 regions where the signal intensity drops by 20% or more compared to its immediate surroundings, a finding in good agreement with the expected cell count. It is possible that there is some overlapping between labeled cells and that some labeled cells do not provide enough contrast to be detected. Other samples with differing concentrations of T cells have yielded similar results (results not shown).

Comparison between MR and fluorescence microscopy images

In a further attempt to confirm that the dark regions are due to the SPIO particles residing in T cells and not air bubbles or free SPIO particles, samples were prepared containing SPIO-labeled T cells colabeled with DiI. Fig. 6 *A* shows an MR image of a microscope slide containing a sample of T cells colabeled with SPIO and DiI. Fig. 6 *B* shows a fluorescence microscopic image of the same sample. An overlay of the two images in Fig. 4 *C* shows strong correlations between the two different sets of images. It should be noted that the labeling efficiency achieved for the SPIO particles is approximately 20% using our present procedure, whereas that of the DiI is near 100%. This means that MR images will indicate fewer cells than fluorescence microscopy, although general distributions should be similar. Note that cells look larger in MRI due to the fact that iron oxide particles appear at least 50$\times$ larger than their actual size due to a large susceptibility effect generated by SPIO particles (Lauterbur et al., 1986). MR images of samples labeled only with DiI showed no contrast.

DISCUSSION

Using the model system of T cells, we have visualized single SPIO-labeled cells by MRI. Labeling T cells through endocytosis has an advantage in that the labeling particles are collected in the phagocytic vacuoles and act essentially as a larger superparamagnetic particle. The dimensions of the phagocytic vacuole are much smaller than the dimensions of the imaging voxel such that the particle collection can be considered a point source creating a localized field larger than the field created by an even distribution of single particles. This is of particular benefit for high-resolution imaging, where regional variations become apparent instead of being averaged over a larger sample volume as in the case

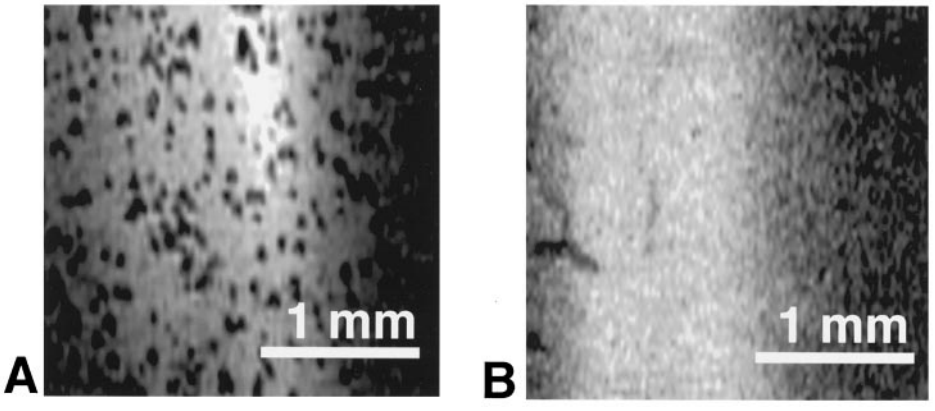

FIGURE 5 (*A*) MR image of microscope slide containing 10 $\times$ 10^6 SPIO-labeled T cells/ml in 3% gelatin. (*B*) MR image of microscope slide containing free SPIO sample (1.0 μg Fe/ml) with twice the amount of iron as the previous T cell sample labeled with SPIO particles. Imaging parameters were as follows: Gradient-echo image TR/TE = 1000/40 ms; FA = 45°; acquisition bandwidth = 15 kHz; NA = 32 for the labeled sample and 64 for the unlabeled sample; imaging time = 2 h for the labeled sample and 4 h for the free SPIO sample.

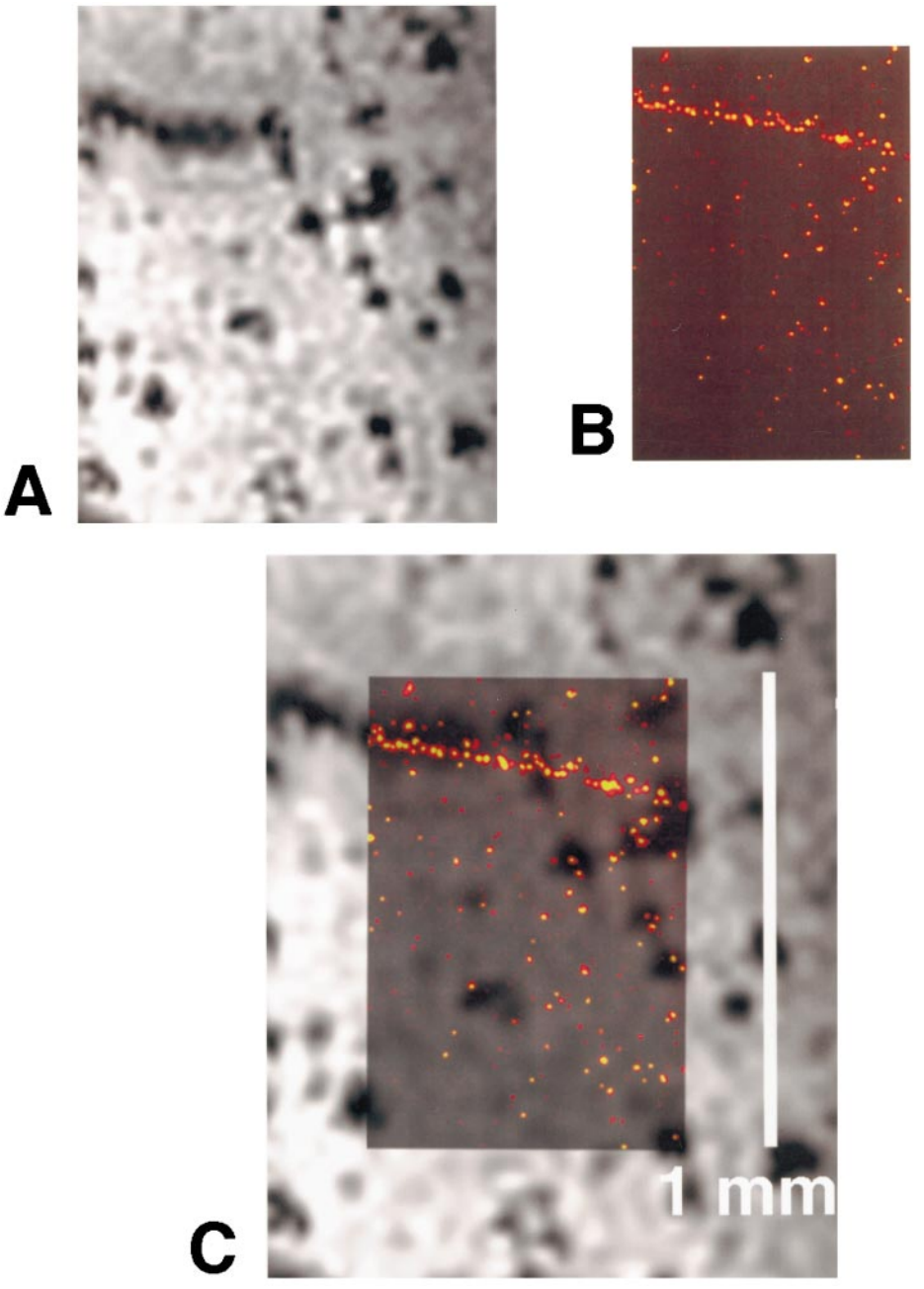

FIGURE 6 MR image of a microscope slide containing T cells colabeled with SPIO and DiI (*A*), fluorescence image of the same microscope slide (*B*), and a comparison of the two images (*C*).

of an even distribution of particles. Another likely advantage is that labeling through endocytosis will not significantly affect the functional properties of the cells, because the labeling particles reside wholly within the cell and are not attached to the cell exterior, as is the case with other labeling techniques. It has been shown that rat T cells labeled with SPIO by endocytosis retain their functions (Yeh et al., 1993, 1995). In this paper, we have demonstrated the benefit of MR imaging at high spatial resolution and have established conditions for detecting single labeled cells.

Diffusion coefficient values in 3% w/v gelatin were measured to be 10% less than the value for distilled water. Calibrating to the known diffusion coefficient for distilled water, 2.5×10^{-3} mm^2/s, a value of 2.2×10^{-3} mm^2/s is estimated as the diffusion coefficient for water in the gelatin sample. Thus, for an echo time of 30 ms, water will diffuse approximately 11.5 μm. This indicates that diffusion can have a significant blurring effect on the image in the high-resolution studies presented here, although it should not interfere greatly with the detection of the superparamagnetic particles. Diffusion will also enhance the transverse relaxation rate in regions of field inhomogeneities (Hardy and Henkelman, 1991), which, in this case, will be the SPIO-labeled T cells. In the presence of the strong imaging gradients needed for MR microscopy, the apparent T_2 is known to decrease due to self-diffusion effects leading to signal loss (Brandl and Haase, 1994).

Local susceptibility causes the effect of the SPIO-labeled cell on an MR image. Thus, imaging methods which emphasize signal loss due to field inhomogeneities will be

beneficial. Using low gradient strengths through the use of low acquisition bandwidths will also enhance susceptibility effects. Low gradient strengths are also beneficial in high-resolution imaging in terms of signal-to-noise ratio, due to the reduced diffusion losses. Reliable susceptibility values for the SPIO samples are not currently available and thus an accurate estimate of local susceptibility effects on MR images has yet to be performed.

For in vivo imaging, detection of superparamagnetically labeled cells becomes inherently more difficult, with contrast reduced through shorter tissue T_2 values and animal motion and stability imposing limits on these studies. While it is improbable that a single labeled T cell may be readily detected in vivo, it is expected that the accumulation of labeled T cells in small localized areas will be detectable. The method of using endocytosis to label cells with MRI contrast agents and carrying out high-resolution MRI should be applicable to systems where cells are concentrated. For example, T cells accumulate in large number in areas of organ rejection. With resolutions on the order of 250 μm, these accumulations should be readily detected. This resolution is achievable in rat studies and, with the advent of high-field human MRI, should be achievable in patients. Another advantage of using high-resolution MRI is that artifacts due to large susceptibility boundaries, such as tissue boundaries in animals, are reduced while at the same time, the local contrast obtained with the SPIO-labeled cells is increased.

CONCLUSION

Using superparamagnetic iron oxide particles that accumulate in T cells of rats via endocytosis, we have shown that single T cells can be detected by high-resolution MRI. The key is that small iron oxide particles accumulate in phagocytic vacuoles in the cell, acting like a much more effective contrast agent due to a large susceptibility effect generated by the sequestered SPIO particles. This permits the detection of single T cells by MRI at resolutions that can be achieved in vivo in animals and potentially in humans. Comparisons between fluorescence microscopic and MR images show similar distributions of cells, indicating that the SPIO particles are resident in the T cells. Our approach to tracking cell migration by MRI is a general one. There are many diseases in which infiltration of immune cells is a part of the pathophysiology and our approach should enable specific diagnosis and monitoring of treatment. Thus, our methodology can be applied to monitor the movement of any type of cell using a modern MRI instrument, provided that sufficient amounts of a suitable MRI contrast agent can be incorporated into the cells and that this process does not alter the functional properties of the cells being labeled.

Some of the results presented in this paper were presented at the 6th Scientific Meeting and Exhibition of the International Society for Magnetic Resonance in Medicine held April 18–24, 1998 in Sydney, Australia. We thank Drs. Paul C. Lauterbur, Irving J. Lowe, Ralph Weissleder, Suzanne T. Ildstad, Christina L. Kaufman, Pedro J. del Nido, and E. Ann Pratt for helpful discussions. We are grateful to Dr. Leaf Huang of the Department of Pharmacology, University of Pittsburgh School of Medicine, for providing the laser light-scattering measurements of our samples of dextran-coated iron oxide particles and to Dr. Charles A. Ettensohn and Mr. Paul G. Hodor of the Department of Biological Sciences, Carnegie Mellon University, for assisting us with fluorescence microscopic measurements of our T cell samples. This work was supported by research grants from the National Institutes of Health (P41RR-03631 and R01RR-10962) and the Whitaker Foundation.

REFERENCES

Brandl, M., and A. Haase. 1994. Molecular diffusion in NMR microscopy. *J. Magn. Reson.* 103B:162–167.

Bulte, J. W. M., Y. Hoekstra, R. L. Kamman, R. L. Magin, A. G. Webb, R. W. Briggs, K. G. Go, C. E. Hulstaert, S. Miltenyi, T. H. The, and L. de Leij. 1992. Specific MR imaging of human lymphocytes by monoclonal antibody-guided dextran magnetite particles. *Magn. Reson. Med.* 25:148–157.

Callaghan, P. T. 1990. Susceptibility-limited resolution in nuclear magnetic resonance microscopy. *J. Magn. Reson.* 87:304–318.

Dubois, M., K. A. Gilles, J. K. Hamilton, P. A. Rebers, and F. Smith. 1956. Colorimetric methods of determination of sugars and related substances. *Anal. Chem.* 28:350–356.

Ghosh, P., N. Hawrylak, J. Broadus, W. T. Greenough, and P. C. Lauterbur. 1990. NMR imaging of transplated iron-oxide-labeled cells in the rat brain. Proc. of the Society of Magnetic Resonance in Medicine, 9th Annual Meeting, New York, p. 1193.

Hardy, P., and R. M. Henkelman. 1991. On the transverse relaxation rate enhancement induced by diffusion of spins through inhomogeneous fields. *Magn. Reson. Med.* 17:348–356.

Lauterbur, P. C., M. L. Bernardo, Jr., M. H. Mendonca Dias, and L. K. Hedges. 1986. Microscopic NMR imaging of the magnetic field around magnetic particles. Proc. of the Society of Magnetic Resonance in Medicine, 5th Annual Meeting, Montreal, Quebec, Canada, pp. 229–230.

Litvin, D. A., and D. L. Rosensireich. 1984. Separation of lymphoid cells on nylon wool columns. *Methods Enzymol.* 108:298–302.

Molday, R. S., and D. Mackenzie. 1982. Immunospecific ferromagnetic iron-dextran reagents for the labeling and magnetic separation of cells. *J. Immunol. Methods.* 52:353–367.

Palmacci, S., and L. Josephson. 1993. Synthesis of polysaccharide covered superparamagnetic oxide colloids (example 1). U. S. Patent 5,262,176. 16 November 1993.

Papisov, M. I., A. Bogdanov, Jr., B. Schaffer, N. Nossif, T. Shen, R. Weissleder, and T. J. Brady. 1993. Colloidal magnetic resonance contrast agents: effect of particle surface on biodistribution. *J. Magnetism and Magnetic Materials.* 122:383–386.

Picker, L. J., and E. C. Butcher. 1992. Physiological and molecular mechanisms of lymphocyte homing. *Annu. Rev. Immunol.* 10:561–591.

Schoepf, U., E. M. Marecos, R. J. Melder, R. K. Jain, and R. Weissleder. 1998. Intracellular magnetic labeling of lymphocytes for in vivo trafficking studies. *BioTechniques.* 24:642–651.

Weissleder, R., A. S. Lee, B. A. Khaw, T. Shen, and T. J. Brady. 1992. Antimyosin-labeled monocrystalline iron-oxide allows detection of myocardial infarct: MR antibody imaging. *Radiology.* 182:381–385.

Weissleder, R., H. Cheng, A. Bogdanova, and A. Bogdanov. 1996. Magnetically labeled cells can be detected by MR imaging. *J. Magn. Reson. Imaging.* 7:258–263.

Yeh, T.-c., W. Zhang, S. T. Ildstad, and C. Ho. 1993. Intracellular labeling of T-cells with superparamagnetic contrast agents. *Magn. Reson. Med.* 30:617–625.

Yeh, T.-c., W. Zhang, S. T. Ildstad, and C. Ho. 1995. In vivo dynamic MRI tracking of rat T-cells labeled with superparamagnetic iron-oxide particles. *Magn. Reson. Med.* 33:200–208.